Monitoring of Sierra Nevada Caves Reveals the Potential for Stalagmites to Archive Seasonal Variability

Barbara E. Wortham[1]*, Isabel P. Montañez[2], Kimberly Bowman[3], Daphne Kuta[2], Nora Soto Contreras[2], Eleana Brummage[2], Allison Pang[2], John Tinsley[4] and Greg Roemer-Baer[4]

[1]Department of Earth and Planetary Science, University of California, Berkeley, Berkeley, CA, United States, [2]Department of Earth and Planetary Sciences, University of California, Davis, Davis, CA, United States, [3]Department of Water Resources, West Sacramento, CA, United States, [4]The Cave Research Foundation, Fresno, CA, United States

In the southwestern United States, California (CA) is one of the most climatically sensitive regions given its low ($\leq$250 mm/year) seasonal precipitation and its inherently variable hydroclimate, subject to large magnitude modulation. To reconstruct past climate change in CA, cave calcite deposits (stalagmites) have been utilized as an archive for environmentally sensitive proxies, such as stable isotope compositions (δ^{18}O, δ^{13}C) and trace element concentrations (e.g., Mg, Ba, Sr). Monitoring the cave and associated surface environments, the chemical evolution of cave drip-water, the calcite precipitated from the drip-water, and the response of these systems to seasonal variability in precipitation and temperature is imperative for interpreting stalagmite proxies. Here we present monitored drip-water and physical parameters at Lilburn Cave, Sequoia Kings Canyon National Park (Southern Sierra Nevada), CA, and measured trace element concentrations (Mg, Sr, Ba, Cu, Fe, Mn) and stable isotopic compositions (δ^{18}O, δ^2H) of drip-water and for calcite (δ^{18}O) precipitated on glass substrates over a two-year period (November 2018 to February 2021) to better understand how chemical variability at this site is influenced by local and regional precipitation and temperature variability. Despite large variability in surface temperatures and precipitation amount and source region (North Pacific vs. subtropical Pacific), Lilburn Cave exhibits a constant cave environment year-round. At two of the three sites within the cave, drip-water δ^{18}O and δ^2H are influenced seasonally by evaporative enrichment. At a third collection site in the cave, the drip-water δ^{18}O responds solely to precipitation δ^{18}O variability. The Mg/Ca, Ba/Ca, and Sr/Ca ratios are seasonally responsive to prior calcite precipitation at all sites but minimally to water-rock interaction. Lastly, we examine the potential of trace metals (e.g., Mn^{2+} and Cu^{2+} as a geochemical proxy of recharge and find that variability in their concentrations has high potential to denote the onset of the rainy season in the study region. The drip-water composition is recorded in the calcite, demonstrating that stalagmites from Lilburn Cave, and potentially more regionally, could record seasonal variability in weather even during periods of substantially reduced rainfall.

Keywords: karst, drip water geochemistry, trace element (TE), oxygen isotope (δ18O), cave monitoring

INTRODUCTION

The monitoring of caves and surface environments (the karst system) is an important approach for understanding processes that impact paleoclimate proxy records developed using cave calcite deposits ("speleothems"). Monitoring the cave environment allows for a quantification of the impact of temperature, precipitation and CO_2 variability, and cave processes on stable isotopic compositions ($\delta^{18}O$, δ^2H, $\delta^{13}C$) and trace element concentrations (Mg, Ba, Sr, etc.), commonly applied proxies in stalagmite paleoclimate reconstruction (McDermott, 2004; Wong and Breecker, 2015). For example, precipitation source, precipitation amount, and precipitation type (i.e., snow or rainfall), as well as relative humidity, and temperature all can influence drip-water and stalagmite $\delta^{18}O$ values (Banner et al., 2007; Fairchild and Baker, 2012; Oster et al., 2012; Luo et al., 2014; Baker et al., 2019). Furthermore, studies have shown that vegetation density and wildfire activity can impact hydrologic recharge to a cave system leading to drip-water $\delta^{18}O$ variability (Nagra et al., 2016; Treble et al., 2016; McDonough et al., 2021). Trace element variability (Mg/Ca, Sr/Ca, and Ba/Ca) and $\delta^{13}C$ compositions are also influenced by precipitation amount as well as bedrock composition and pCO_2 ventilation regimes in a cave (Fairchild and Treble, 2009; Wong et al., 2011; Oster et al., 2012; Oster et al., 2014; Casteel and Banner, 2015; Oster et al., 2015). Therefore, inferring environmental conditions from stalagmite geochemical compositions is complicated by the confounding effects of multiple influences on their signatures (Lachniet, 2009; Fairchild and Baker, 2012). This reflects the fact that geologic and hydrologic conditions of the karst system (i.e., soil, epikarst, and cave) control how the climate signal is transferred to the geochemical compositions of the drip-water and mineral precipitate as well as their included fluids (e.g., Dreybrodt and Scholz, 2011; Tremaine et al., 2011; Feng et al., 2014). As a result, the proxy signals can be dampened, enhanced, or biased by karst processes, and predominant environmental influence(s) can vary by cave, within a region, and by drip site within a single cave (Hendy, 1971; Mickler et al., 2004; Fleitmann et al., 2009; Markowska et al., 2015; Mickler et al., 2019). Thus, spatial variability in drip-water and stalagmite geochemical compositions can potentially be unrelated to the external climate signal.

In addition, recent studies have further documented that stalagmites are robust archives of paleo-fire activity (e.g., Nagra et al., 2016; Treble et al., 2016; Bian et al., 2019). Given the more than doubling of extreme seasonal fire weather conditions in CA over the past 4 decades (Goss et al., 2020), there is an opportunity to integrate fire-derived proxies into cave monitoring studies in fire-prone regions. Despite the clear research benefits of monitoring cave systems from which stalagmite-based reconstructions are developed, there have been only three cave monitoring studies in California (Oster et al., 2012; Oster et al., 2017; Oster et al., 2020).

Here we present 2 years of monitoring data from Lilburn Cave in Sequoia and Kings Canyon National Parks (herein referred to as "SEKI"). The resul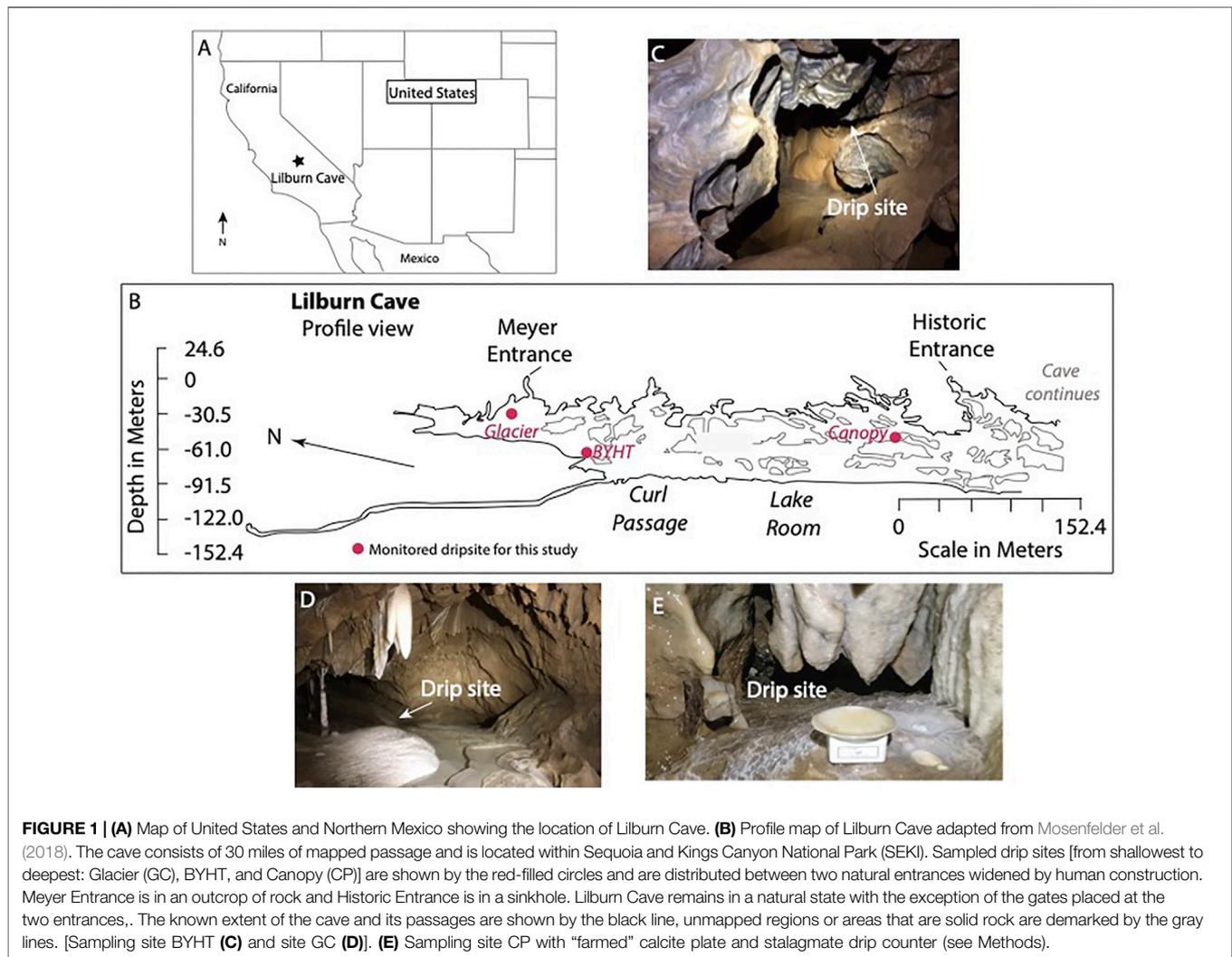ts from this study are integrated with cave monitoring and precipitation data from Black Chasm (Oster et al., 2012), precipitation monitoring data from SEKI (McCabe-Glynn et al., 2016). Additionally, the results are compared to modeled drip-water and stalagmite $\delta^{18}O_{cc}$ time series, which were produced using the forward proxy system model, Karstolution (Treble et al., 2019). This study provides a monitoring framework that is applicable more broadly to stalagmite studies from other seasonally dry karst systems. Notably, this work was done as part of a vertically integrated mentoring program in which a diverse group of undergraduate researchers were taught theoretical science through experiential learning in the classroom, the lab and in the field (www.blogofbarbarawortham.com). In turn, the undergraduate researchers developed hypothesis-driven research projects as undergraduate theses and mentored younger undergraduate students in the field and in the lab. The data presented here is from these research projects and this article represents a culmination of that effort into one coherent study.

SITE DESCRIPTION

Lilburn Cave, in the Kings Canyon NP portion of SEKI, is hosted in a northwest-southeast trending band of Mesozoic marble bounded by relatively insoluble granite and granodiorite (Tobin and Schwartz, 2012). The majority of Lilburn Cave is developed in calcite marble, although dolomitic marble and limy dolomite marble have been observed (Tinsley et al., 1981). The cave occurs in Redwood Canyon through which Redwood Creek submerges underground to the lowest level of Lilburn Cave, and ultimately resurfaces at Big Spring. Multiple smaller streams feed Redwood Creek throughout the watershed (Tobin and Schwartz, 2012).

In this study of Lilburn Cave, we monitored three drip-water sites, at different levels within the cave, from May 2018 through February 2020 (**Figure 1**). At the shallowest site, Glacier (GC) (~30 m to surface/entrance), a stalactite feeds a small stalagmite and rim pool. We sampled water from the rim pool at the GC site that is directly fed by the stalactite drip. Big Yellow Hungus Thing (BYHT) occurs at mid-level in Lilburn Cave (~61 m below surface) and is a flowstone that is fed by pools, which receive drip-water from the cave ceiling. We sampled BYHT from a 6-inch-wide pool fed directly from the cave ceiling. The third site, Canopy (CP), is closest to the historic entrance in the cave (a sinkhole), is ~61 m from surface, and has a stalagmite fed by drip-water sourced from the cave ceiling (**Figure 1**).

The climate of SEKI is mediterranean with cool wet winters and warm summers. Precipitation is greater in higher elevations in the southern Sierra Nevada, although there is a smaller range in the south than in the northern Sierra Nevada) (Caprio and Lineback, 1997). The climatology from 1981 to 2010 demonstrates that lower elevations in SEKI receive 900–1,000 mm of precipitation annually, whereas higher peaks receive 1,270–1,524 mm (PRISM, 2021). Additionally, annual average temperature from 1981 to 2010 varies from 3.9 to 6.1°C (PRISM, 2021). Snow accumulations in winter are common above 1,515 m (Caprio and Lineback, 1997). Over

FIGURE 1 | (A) Map of United States and Northern Mexico showing the location of Lilburn Cave. **(B)** Profile map of Lilburn Cave adapted from Mosenfelder et al. (2018). The cave consists of 30 miles of mapped passage and is located within Sequoia and Kings Canyon National Park (SEKI). Sampled drip sites [from shallowest to deepest: Glacier (GC), BYHT, and Canopy (CP)] are shown by the red-filled circles and are distributed between two natural entrances widened by human construction. Meyer Entrance is in an outcrop of rock and Historic Entrance is in a sinkhole. Lilburn Cave remains in a natural state with the exception of the gates placed at the two entrances,. The known extent of the cave and its passages are shown by the black line, unmapped regions or areas that are solid rock are demarked by the gray lines. [Sampling site BYHT **(C)** and site GC **(D)**]. **(E)** Sampling site CP with "farmed" calcite plate and stalagmate drip counter (see Methods).

the monitoring period (2018–2021), the precipitation at Grant Grove Ranger station ranged from 0 to 400 mm with snow accumulation from December through May, typically (WRCC, 2021). Previous studies demonstrate that the Sierra Nevada receive rainfall from the N. Pacific and from the subtropical Pacific (Oster et al., 2009; Oster et al., 2015; McCabe-Glynn et al., 2016).

METHODS

Monitoring at Lilburn Cave sites began in May of 2018. Drip-water was sampled and cave pCO_2 was measured monthly through March of 2020 after which the National Park restrictions in response to the COVID-19 pandemic precluded further access to the cave. Winter sampling (January–May) of Lilburn Cave is excessively difficult due to depth of snowpack and National Park road conditions and/or road closures. Instruments to automatically record cave-air pCO_2 (Vaisala M170), relative humidity (RH) and temperature (Onset HOBO logger model Pro V2) were placed at BYHT from 2018 through 2019. Automated

measurements were made throughout this monitoring period. Temperature (via thermometer) and pCO_2 were spot measured by hand every month at GC and CP. Automatic measurements of drip rates (Stalagmate Drip Counter from Driptych) were made at the CP and GC sites throughout 2019. Automated measurements were taken every 12 h between cave trips and were verified with spot measurements during monthly visits. We sampled drip-water at each site for $\delta^{18}O$ and δ^2H and trace element (herein referred to as TE) analysis and for pH, and alkalinity measurements (details in **Section 2**) following the methods of Wong et al. (2011) and Oster et al. (2012). Three water samples were taken at each site during monthly visits: drip-water was collected in 1) clean HDPE 15 ml bottles for TE analysis, 2) clean 2 ml glass vials for $\delta^{18}O/\delta^2H$ analysis, and 3) clean 20 ml amber glass vials for alkalinity and pH analysis.

Additionally, surface water samples at the creeks and streams in Redwood Canyon were taken in 2018 and 2020 following the aforementioned protocol and snow samples were obtained in February 2019 and February 2020 following the protocol of Earman et al. (2006). Snow was sampled by digging trenches

in snow drifts at the North end of Redwood Canyon and sampling at 6-inch intervals to the ground surface (**Supplementary Figure S1**). Snow samples were sealed in clean sampling bags and taken back to the Sedimentary Geochemistry Lab at UC Davis, where they were slowly melted in sealed containers at room temperature and subsequently sampled as water for analysis.

To understand how the drip-water signal is imprinted in the stalagmite calcite, we placed two sanded watch glasses (10 cm diameter) under the drip at the CP and GC sties (**Figure 1**) in November 2018. Watch-glass plates were used to initiate calcite growth on a material that could be sampled using the approach of Banner et al. (2007). The watch glasses were retrieved in February 2021 and the calcite on each plate was subsampled for analysis of stable isotopic compositions ($\delta^{18}O$ and $\delta^{13}C$), TE and trace metal concentrations. The watch glass from CP was sampled five times along a transect from the center to edge of the calcite growth on the plate, mimicking the subsampling of a stalagmite from the proposed "growth axis" to the outer "flank" of the stalagmite.

The stable isotopic compositions ($\delta^{18}O$ and δ^2H) of drip-waters were analyzed at the Stable Isotope Facility, University of California, Davis (UC Davis), and calcite $\delta^{18}O$ and $\delta^{13}C$ were analyzed at the Stable Isotope Lab, UC Berkeley. TE concentrations of waters and calcites (Sr, Mg, Ba, Fe, Mn, etc.) were analyzed at the Interdisciplinary Center for Plasma Mass Spectrometry, UC Davis).

To better understand the drip-water and calcite data, we used the forward model Karstolution (Treble et al., 2019) and the precipitation data from SEKI, measured between 2001 and 2011 (McCabe-Glynn et al., 2016), as well as from Black Chasm (Oster et al., 2012) to simulate drip-water and calcite $\delta^{18}O$ compositions for the Lilburn karst system. We compared the modeled $\delta^{18}O$ time series to the measured values of Lilburn Cave drip-water and stalagmite calcite. Additionally, we calculated a series of threshold ratios for Mg/Ca, Sr/Ca, and Ba/Ca to determine the influence of water-rock interaction (WRI), prior-calcite precipitation (PCP), as well as to assess evidence for incongruent dolomite or calcite dissolution (IDD), following the methods of Sinclair (2011), Sinclair et al. (2012), and Casteel and Banner (2015). We compared these results to thresholds empirically derived concentrations calculated using K_D values for Mg, Sr, and Ba (Sinclair, 2011; Sinclair et al., 2012; Casteel and Banner, 2015).

RESULTS

## Results of Lilburn Cave Drip-Water and Calcite Measurements

For all three Lilburn cave sites, air pCO_2, RH, and temperature remain constant throughout the year (Summary: 678 +/− 43 ppm, 100% humidity, 7.4°C; **Supplementary Table S1**). A typical period between when automated sampling devices were deployed and retrieved is shown in **Supplementary Figure S2**. Drip rates at BYHT were not recorded when sampling as the drip-water flowed continuously from the ceiling of the cave to the top of a flowstone. At the nearest site to the entrance, GC (**Figure 1**), the drip rate ranges from the highest recorded value (six drips/second) during March to May and decreases to the lowest values (<1 drips/second)

throughout the summer and into the early winter months (June through December) (**Figure 2**). At CP (**Figure 1**), drip rates range from one to three drips/second, with the highest drip rates occurring between March to May (**Figure 2**) and the lowest during August through December. All stable isotope and trace element results are tabulated in **Supplementary Table S2**. Seasonally, the drip-water $\delta^{18}O$ compositions are similar at GC and CP, with the highest values occurring during the autumn and early winter months (September–December). In contrast, BYHT drip-water $\delta^{18}O$ compositions reach their lowest values in autumn and early winter (September–December) and rise to their highest values in the spring (March–May) (**Figure 3**). The single $\delta^{18}O$ measurement of "farmed" calcite grown *in situ* at GC is -8.7‰ and the $\delta^{18}O$ of calcite at CP ranges between −8.6 and −9.4‰ (±0.06%).

Drip-water $\delta^{18}O$ and δ^2H values for Lilburn Cave define a slope and intercept ($\delta^2H = 6.5 * \delta^{18}O - 3.4$) that lie between those defined by precipitation compositions from SEKI ($\delta^2H = 7.6 * \delta^{18}O + 8.5$), and of surface water from Redwood Canyon ($\delta^2H = 5.4 * \delta^{18}O - 17.8$) (**Figure 4**). We compare the slopes of drip-water $\delta^{18}O$ and δ^2H compositions to that of precipitation from SEKI for 2001 to 2011 (McCabe-Glynn et al., 2016) as well as to snow and surface water compositions from Redwood Canyon sampled during the period of cave monitoring (**Figure 4**). The slope for the drip water at Lilburn Cave falls between that of the SEKI precipitation and the Redwood Creek stream water. Drip-water compositions do appear to not represent precipitation or surface water alone.

Seasonally, the TE/Ca ratios for CP and BYHT decrease in the autumn, contemporaneously with the increase in autumn precipitation in SEKI (**Figure 4**). The decrease of drip-water TE/Ca ratios at BYHT in the autumn is contemporaneous with a decrease in the $\delta^{18}O$ compositions. Alternatively, the decrease in TE/Ca ratios at CP occurs when $\delta^{18}O$ compositions are increasing. The signatures at GC, however, reveal that drip-water TE/Ca ratios at this site increase in the autumn and mirror an increase in $\delta^{18}O$ compositions (**Figure 4**). The TE/Ca ratios at the three sites each respond differently to the variability in SEKI precipitation. To further examine the source of this variability, we analyzed the relationship between Ba, Sr, and Mg using the approach of Sinclair (2011), Sinclair et al. (2012), and Casteel and Banner (2015). A cross-plot of ln (Mg/Ca), ln (Sr/Ca), and ln (Ba/Ca) ratios in the drip-water of each cave site exhibits calculated slopes that range from 0.8 to 1.1 (**Figure 5**). The Black Chasm drip water slope for Mg/Ca and Sr/Ca is 0.99 (**Figure 5**). Values of Ba/Ca were not measured for Black Chasm.

The TE concentrations from the calcite grown *in situ* at Lilburn Cave are comparable (taking into account K_Ds) to the drip-water concentrations at GC and CP. Sr, Mg, and Ba concentrations in the *in situ* precipitated calcite at the shallowest and furthest sites from the Meyer Entrance (GC and CP, respectively) are comparable to those of the drip-waters from these sites (**Supplementary Table S2**). The concentrations of Mg at these Lilburn Cave sites range from 4,230 to 4,456 ppb at CP and 23989 to 2,790 ppb at GC as compared to 1,092 ppb and 701 ppb in the calcite from CP and GC, respectively. The Sr concentrations in the drip-water at these sites range between 190 and 196 ppb at CP and 110–128 ppb at GC as compared to
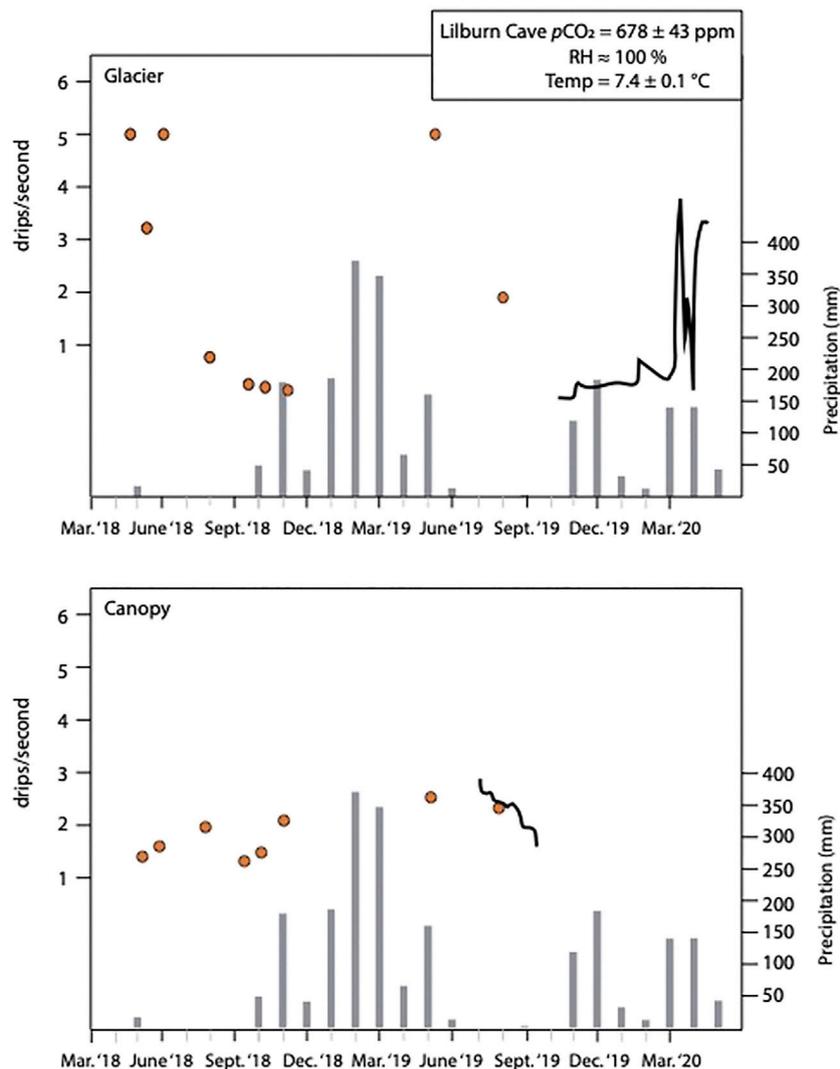
FIGURE 2 | Water data from Lilburn Cave and SEKI for 2018 to 2020. Drip rate counts at Glacier and Canopy sites as spot (orange dots) and automated (black line) measurements plotted against monthly precipitation amount (grey bars) for Grant Grove Ranger Station, SEKI. Sampling at Lilburn Cave in the winter was limited by National Park road conditions and snow levels in SEKI. Lilburn Cave pCO_2, RH, and temperature results from the automated measurements are summarized in the inset and represent the monitored portion of the cave. Spot measurements **Supplementary Table S1**. A typical log file for automated measurements is shown in **Supplementary Figure S3**.

191 and 183 in the farmed calcite from CP and GC, respectively. The concentrations of Ba at these drip sites range between 89 and 102 ppb at GC and between 74 and 83 ppb at CP as compared to 68 and 154 ppb in the farmed calcite from GC and CP, respectively.

The concentrations of less commonly applied trace metals (Cu^{2+}, Mn^{2+}, Fe^{3+}) in the Lilburn drip waters were examined to determine their viability as a new geochemical signal of seasonal recharge in this cave. To evaluate these elements, we compared the seasonal trend in their concentrations in the drip water to the precipitation amount in SEKI. Mn^{2+} concentrations in the shallowest and intermediate depth sites (GC and BYHT) vary seasonally with minimum values (0.0–1.5 ppb) in the spring and summer that increase 2 to 6-fold in autumn (0–3.0 ppb) contemporaneously with an increase in

precipitation amount (**Figure 6**). In contrast, the Mn^{2+} concentration at CP is more variable, although there is a rise in values contemporaneous with an increase in precipitation amount, comparable to the other two sites (**Supplementary Table S2**). Cu^{2+} concentrations at all three drip sites exhibit a similar seasonal trend to Mn^{2+} concentrations and increase in concentration in the drip-water synchronous with an increase in precipitation amount. One notable exception is that Cu^{2+} concentrations at all three drip sites double in August of 2019 relative to August 2018 concentrations (**Figure 6**). Fe^{3+} concentrations at all three drip sites are more variable with overall low values through 2018 (~5–10 ppb for the bulk of the dataset) but increase overall (range of ~10.0–60.0 ppb) in 2019. Concentrations of all three metals in the "farmed" calcite at CP (Mn = 4 ppb, Fe = 223 ppb, and Cu = 2.4 ppb) and at GC (Mn =
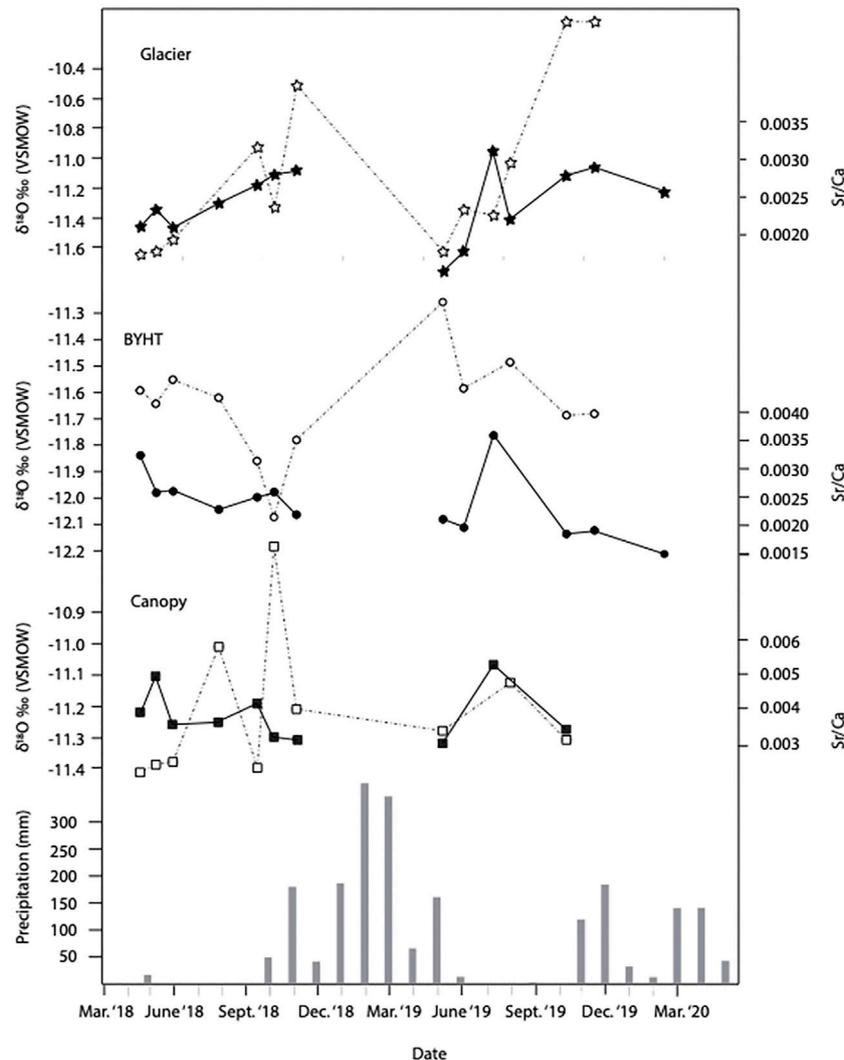
FIGURE 3 | Sr/Ca ratios and δ^{18}O compositions for the three Lilburn drip-sites. Sr/Ca ratios (filled symbols) are plotted alongside δ^{18}O compositions (open symbols) for the Glacier (stars), BYHT (circles), and Canopy (squares) sites. Precipitation amount (as in **Figure 2**) ranges from 0 in to 16 inches per month.

2 ppb, Fe = 66 ppb, Cu = 22 ppb) are 10-fold higher overall than drip-water concentrations (ranges listed above; **Supplementary Table S2**) accountable by their K_D values.
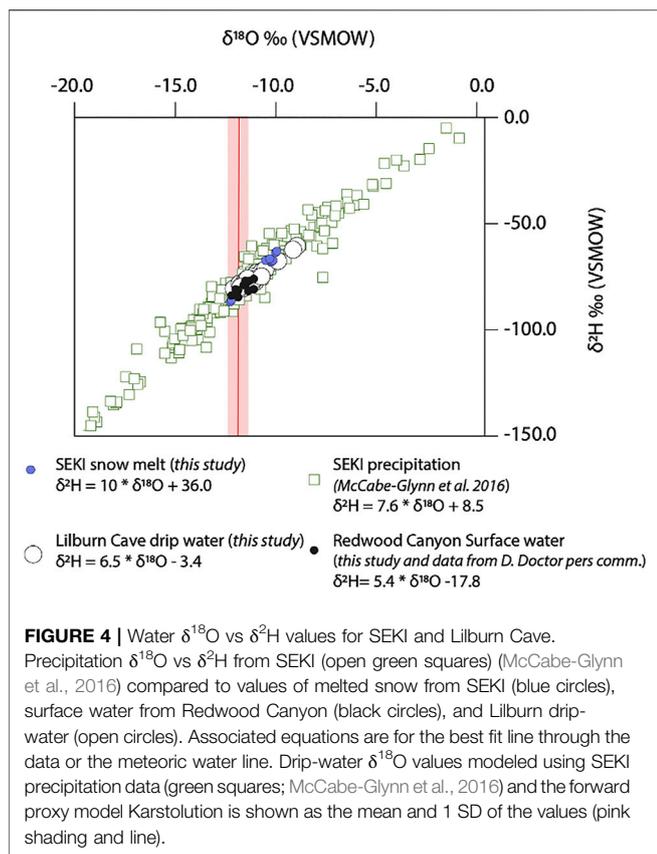
Results From a Previous Cave Monitoring Project in the Central Sierra Nevada, California

To further interrogate the Lilburn Cave monitoring results, we compare the data to a five-year cave monitoring dataset from Black Chasm, a cave from the foothills (elevation of 300 m) of the central Sierra Nevada (Oster et al., 2012). To summarize that study, 5 years of drip water monitoring at five sites in Black Chasm, as well as surface monitoring, revealed that Black Chasm has an average temperature of 12.3°C, with 5°C annual variability (Oster et al., 2012). The pCO$_2$ at Black Chasm ventilates seasonally when cold dense air displaces summer air in the autumn. The relative

humidity at Black Chasm varies seasonally but remains >80% through most of the year. Seasonally, the δ^{18}O of Black Chasm drip water varies in response to changes in precipitation δ^{18}O, with a lag of ~3 weeks, and the precipitation δ^{18}O varies depending on precipitation source and temperature. The δ^{13}C and TE/Ca results from Black Chasm reveal that seasonal variability in rainfall amount drives prior calcite precipitation (Oster et al., 2012).

DISCUSSION

Cave monitoring data provides insight into drip-water amount and chemistry variability within a cave system, which reflects the variability of the karst system and can be used to interpret changes in the region when coupled with paleoclimate records from stalagmites. The monitoring data for Lilburn Cave demonstrates that although the cave air conditions (pCO$_2$, RH,
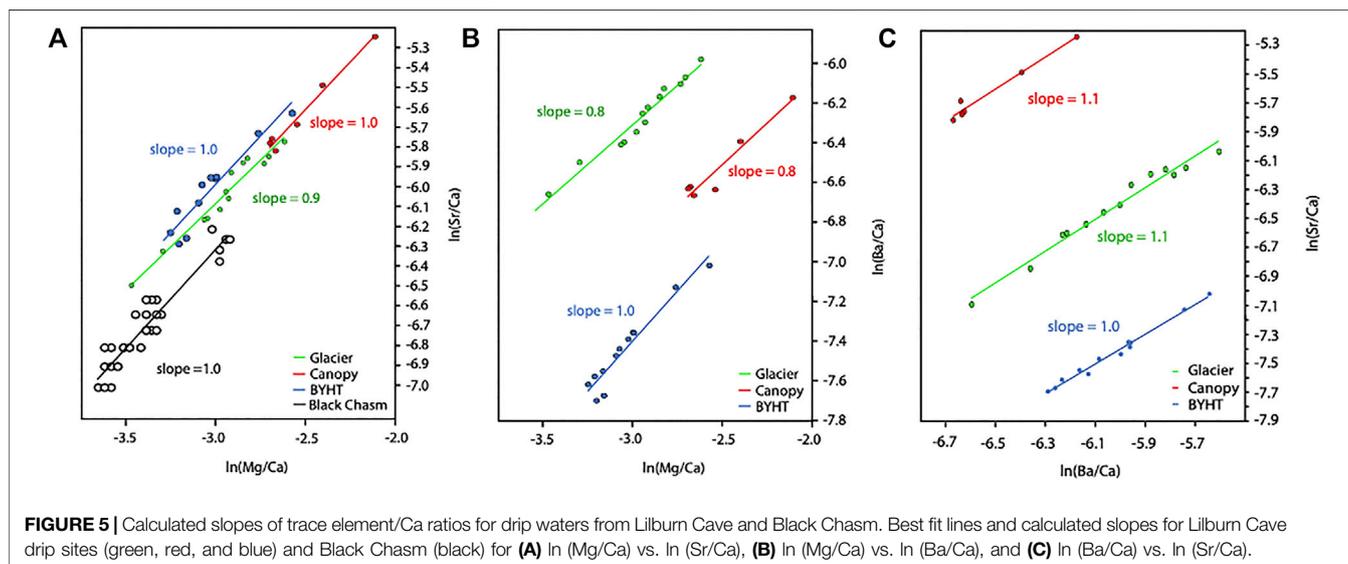
FIGURE 4 | Water $\delta^{18}O$ vs δ^2H values for SEKI and Lilburn Cave. Precipitation $\delta^{18}O$ vs δ^2H from SEKI (open green squares) (McCabe-Glynn et al., 2016) compared to values of melted snow from SEKI (blue circles), surface water from Redwood Canyon (black circles), and Lilburn drip-water (open circles). Associated equations are for the best fit line through the data or the meteoric water line. Drip-water $\delta^{18}O$ values modeled using SEKI precipitation data (green squares; McCabe-Glynn et al., 2016) and the forward proxy model Karstolution is shown as the mean and 1 SD of the values (pink shading and line).
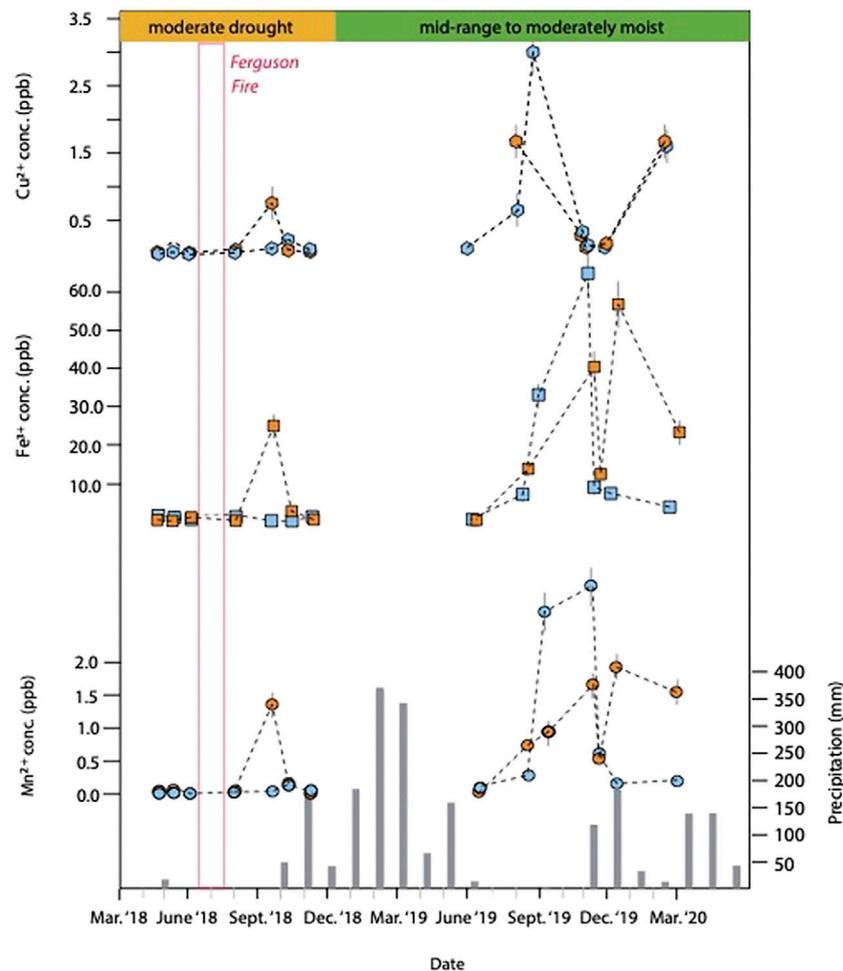
and temperature) remain constant throughout the year, drip rate and the stable isotopic and geochemical compositions of drip waters vary seasonally. We discuss below the seasonal variability at each drip site, integrating each geochemical signal to interpret what process (temperature, precipitation amount, etc.) the drip site may be responding to. Furthermore, we compare the results from this study to drip-water $\delta^{18}O$ compositions and

measurements from another monitoring study at Black Chasm to assess the latitudinal differences along the Sierra Nevada. Finally, we compare how measured and modeled drip-water and calcite values compare to evaluate equilibrium conditions at Lilburn Cave. This allows us to separate drip sites that respond to surface processes and those that respond to in-cave dynamics. Trace metals in drip-water have been tested in recent cave monitoring studies as proxies of aerosol contribution to soil (Tadros et al., 2019), prolonged droughts (Liao et al., 2021), and fire influence on drip-water geochemistry (Nagra et al., 2016; Bian et al., 2019). Below, we evaluate Mn^{2+}, Cu^{2+}, and Fe^{3+} in drip water from Lilburn Cave and its relationship to precipitation amount and drought in SEKI.

Understanding Drip Water Variability

The geochemical variability and drip rates at each drip site in Lilburn Cave reveal seasonal variability related to precipitation amount above the cave, and for GC and CP, airflow regimes in the cave (**Figure 3**). Drip rates at GC and CP increases in response to increased precipitation in the autumn and decreases in response to precipitation loss in the summer, albeit with a 3 months time lag. This relationship indicates that drip rates at these two sites respond to precipitation amount above the cave. Variability in Mg/Ca, Ba/Ca, and Sr/Ca ratios in cave drip waters has been attributed to the type and composition of bedrock, soil composition above the cave, the fluid flow-path through the epikarst (i.e., conduit vs. diffuse), and the change in degree of water-rock interaction driven by water residence time in the epikarst. Additionally, the extent of prior calcite precipitation controlled by both water amount and rate of CO_2 degassing impacts water TE concentrations, which may or may not be governed by the same processes controlling water availability, and the incongruent dissolution of dolomite and/or calcite (Fairchild et al., 2000; Fairchild and Treble, 2009; Sinclair, 2011; Wong et al., 2011; Oster et al., 2012; Sinclair et al., 2012; Casteel and Banner, 2015).

FIGURE 5 | Calculated slopes of trace element/Ca ratios for drip waters from Lilburn Cave and Black Chasm. Best fit lines and calculated slopes for Lilburn Cave drip sites (green, red, and blue) and Black Chasm (black) for **(A)** ln (Mg/Ca) vs. ln (Sr/Ca), **(B)** ln (Mg/Ca) vs. ln (Ba/Ca), and **(C)** ln (Ba/Ca) vs. ln (Sr/Ca).

FIGURE 6 | Trace metals in Lilburn drip water. Mn, Fe, and Cu concentrations for the shallowest site GC (blue symbols) and intermediate site BYHT (orange symbols) plotted with precipitation amount (gray bars) at Grant Grove Ranger Station (SEKI) over the sampling period. Red outlined box is the period of the Ferguson Fire (~160 km away from Lilburn Cave). The Palmer Drought Severity Index for the region of Lilburn Cave (PDSI, 2021) is denoted at the top with a moderate drought extending from March 2018 to Dec. 2018 followed by a mid-range to moderately wet period from January 2019 through to the end of the monitoring period (February 2021).

Based on the aforementioned studies, when the TE/Ca ratios are controlled by water-rock interaction and precipitation amount, it is expected that TE/Ca ratios will increase during periods of lower precipitation amount and higher water-rock interaction and/or prior calcite precipitation. We interpret the seasonal trends in TE/Ca ratios at drip sites in Lilburn Cave as responding directly to prior calcite precipitation and/or water-rock interaction driven by local precipitation amount. At CP and GC, the trends in TE/Ca (see Sr/Ca in **Figure 3**) decrease as drip-rate increases as would be expected if the trend is driven by precipitation amount. The same relationship is also observed at BYHT, although no drip-rate information is available for this site. It is notable, however, that the change in TE/Ca ratios at the GC site lags several months behind the change in precipitation amount in the autumn; this lag is not observed at the CP and BYHT sites (**Figures 2**, **4**) that both exhibit changes in TE/Ca ratios

directly after the changes in precipitation amount in September and/or October.

Although it is useful to understand the seasonal relationship between precipitation amount, drip rate, and TE/Ca, it is not possible to use these trends to tease apart the separate processes of water-rock interaction (WRI) and prior calcite precipitation (PCP). This is because both can cause seasonal variability in TE/Ca values. To address this, we used a mathematical approach that isolates WRI from PCP and assesses the influence on drip-water Mg/Ca, Sr/Ca, and Ba/Ca values (**Figure 5**) (Sinclair, 2011; Sinclair et al., 2012; Casteel and Banner, 2015). Based on this method, the formula $K_{D-Sr}-1/K_{D-Mg}-1$ or $K_{D-Ba}-1/K_{D-Mg}-1$ is used to derive slopes for ln (Mg/Ca) vs ln (Sr/Ca) or ln (Mg/Ca) vs. ln (Ba/Ca) while replacing the K_D values for the appropriate TE/Ca ratio in question. These slopes and the TE data are subsequently used to produce plots that distinguish between PCP or incongruent calcite dissolution (ICD) and WRI in

drip-water values (**Figure 5**) (Sinclair, 2011; Sinclair et al., 2012; Casteel and Banner, 2015). Based on these calculations, the TE/Ca ratios for Lilburn Cave and Black Chasm are driven by PCP or incongruent dolomite or incongruent calcite dissolution. Lilburn Cave is mostly developed in calcite marble, although dolomitic marble and limy dolomite marble have been observed (Tinsley et al., 1981). We cannot rule out the influence of incongruent dissolution of calcite or dolomite, by which trace elements (Mg, Sr, or Ba) are dissolved preferentially and result in increased TE/Ca ratios in the drip water. The observation that Mg, Sr, and Ba concentrations vary in the drip water in the same direction at each site (**Figure 5**) cannot be explained by variability in bedrock composition. We propose that the TE/Ca ratios in Lilburn Cave drip-waters primarily record PCP in the epikarst. Furthermore, the "farmed" calcite TE/Ca values indicate that the calcite directly records drip-water TE/Ca ratios (**Supplementary Table S2**), suggesting the high potential for Lilburn stalagmites to record temporal variability in precipitation amount in this cave.

Variability in the drip-water $\delta^{18}O$ values at the three Lilburn sites further document the influence of seasonal variability in temperature and precipitation, and/or continuous CO_2 ventilation. Notably, the drip-water $\delta^{18}O$ and δ^2H values at all three sites are within the range of the precipitation and snow $\delta^{18}O$ and δ^2H in the region (**Figure 4**). The variability in precipitation $\delta^{18}O$ and δ^2H from 2001 to 2011 reflects the large temperature and source variability in storms that arrive at SEKI. Although the precipitation monitoring period does not overlap with the drip water monitoring period, we assume here that the McCabe-Glynn et al. (2016) dataset is representative of potential precipitation variability through the monitoring 2018 to 2021 in the same area. Alternatively, snow and drip-water $\delta^{18}O$ and δ^2H were not as variable during 2018–2021 in comparison to the period 2001–2011 (**Figure 4**). This is likely due to mixing of precipitation from different storm events in the soil, surface water, or epikarst zone. In comparison, drip-water $\delta^{18}O$ and δ^2H is much less variable than precipitation $\delta^{18}O$ and δ^2H at Black Chasm (**Supplementary Figure S2**; Oster et al., 2012), which is interpreted to be due to mixing in the epikarst.

To better understand the seasonal variability in drip-water $\delta^{18}O$ (**Figure 3**), we modeled annually resolved time series for drip-water $\delta^{18}O$ at Lilburn Cave using Karstolution (Treble et al., 2019) to determine the primary influence(s) on measured $\delta^{18}O$ variability. Karstolution is a forward proxy model that includes measured precipitation $\delta^{18}O$, precipitation amount, evapotranspiration amount, and temperature in its parameterization. Furthermore, Karstolution considers evaporative enrichment of water from the soil zone, however, all other processes in Karstolution assume equilibrium fractionation when the RH is set to 95% humidity, a setting that is relevant for Lilburn Cave. Consequently, although calculated evaporative enrichment of the $\delta^{18}O$ composition at the "modeled" surface of the cave, from the soil zone, may be impacting the drip-water compositions from Karstolution, in-cave kinetic effects are not incorporated into the modeled drip-water compositions in this analysis. The model applies a range of processes of mixing and storage and outputs a time series of drip-water $\delta^{18}O$ compositions and five different time-series of calcite

$\delta^{18}O$. To parameterize Karstolution, we used the 10-years record of precipitation $\delta^{18}O$ composition and amount data from SEKI (McCabe-Glynn et al., 2016) and corresponding temperature and pan evaporation measurements from a nearby weather station (National Oceanic and Atmospheric Administration (NOAA), 2021). The modeled drip-water $\delta^{18}O$ values from Karstolution are similar in composition to the measured $\delta^{18}O$ in drip water from BYHT year-round and are similar to the measured $\delta^{18}O$ of drip water from GC and CP in the spring months (**Figure 7A**). Accordingly, the comparison between the measured drip-water $\delta^{18}O$ and the modeled drip-water $\delta^{18}O$ indicate that the $\delta^{18}O$ compositions at BYHT are representative of the variability in precipitation $\delta^{18}O$ from 2001 to 2011 in SEKI, precipitation amount, temperature, and evaporation (**Figure 7A**). This is a significant result as this behavior suggests that out of the three drip sites monitored at Lilburn Cave, BYHT may be the most ideal to develop a speleothem paleoclimate record that captures precipitation variability in SEKI. In contrast, the $\delta^{18}O$ compositions at GC and CP are experiencing seasonal enrichment (autumn and early winter) as demonstrated by the increased $\delta^{18}O$ in drip water at these sites in comparison to the modeled $\delta^{18}O$ compositions (**Figure 7A**). It is important to note that precipitation monitoring did not occur over Lilburn Cave during the monitoring period and that the increases at GC and CP could reflect variability in precipitation $\delta^{18}O$ in 2018 and 2019 that was greater than the precipitation $\delta^{18}O$ variability captured in the precipitation monitoring effort from 2001 to 2011. However, given that BYHT matches the modeled drip-water $\delta^{18}O$ results closely, we posit that GC and CP are instead influenced by in-cave kinetic effects or dynamics such as increased airflow as they are near the two entrances of the cave (**Figure 1**). Others have found that increased ventilation near entrances potentially leads to variability in $\delta^{18}O$ of calcite (Tremaine et al., 2011; Oster et al., 2012). The enrichment is due to decreased pCO_2 in well ventilated cave passageways that can lead to increase CO_2 degassing from drip water that rapidly changes the $\delta^{18}O$ values of the dissolved inorganic carbonate (DIC) forcing the DIC pool out of equilibrium (Mickler et al., 2004; Mickler et al., 2006; Dreybrodt and Deininger, 2014; Carlson et al., 2020). Additionally, a decrease in cave air RH can lead to increased evaporation from the drip water, forcing the $\delta^{18}O$ values of the water and the DIC pool out of equilibrium (Mickler et al., 2004). These two cave air parameters are the driving cause of is termed in-cave kinetic effects. Cave air pCO_2 and RH remained constant throughout the monitoring period, however, the pCO_2 in Lilburn Cave remained quite low (average of 678 ppm), potentially due to enhanced ventilation and may have led to the increased $\delta^{18}O$ values observed at GC and CP. Although in-cave kinetic effects have been extensively studied (Mickler et al., 2004; Mickler et al., 2006; Riechelmann et al., 2013) they are mainly relegated as a cause for concern or as a reason to disregard a cave, region, or stalagmite sample. The seasonal signal at these two sites, however, can be reframed as a significant finding as the $\delta^{18}O$ enrichment happens in the autumn season of both monitoring years. Future stalagmites taken from Lilburn Cave, given extensive monitoring to determine the relationship between $\delta^{18}O$, airflow, cave air parameters, and
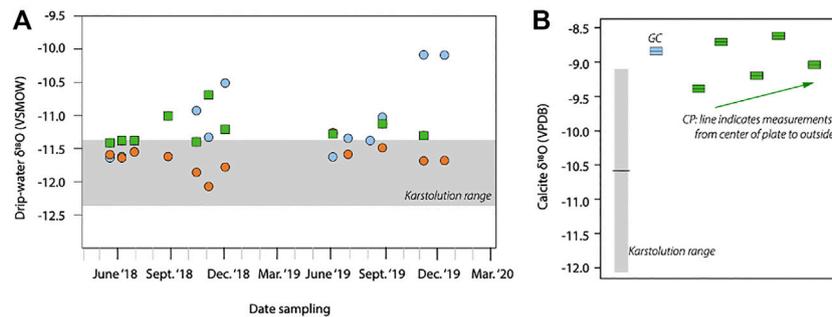
FIGURE 7 | Modeled and measured drip-water $\delta^{18}O$ values for Lilburn Cave. **(A)** Measured drip-water $\delta^{18}O$ values for drip sites GC (blue circles), BYHT (orange circles), and CP (green squares) superimposed on modeled drip water values (gray shading). **(B)** Box plot of modeled calcite $\delta^{18}O$ values (range: gray shading; average: black line) and measured $\delta^{18}O$ values and 1σ uncertainty of calcite grown *in situ* ("farmed") at sites GC (blue box) and CP (green boxes). Green arrow indicates the positionality of the samples on the plate from CP, which are ordered from center **(left)** to outer most edge **(right)**.

precipitation $\delta^{18}O$, could preserve a signal such as that observed at GC and CP that denotes seasonal variability in ventilation. Furthermore, the "farmed" calcite grown *in situ* at Lilburn Cave reveal calcite $\delta^{18}O$ that are similar to the modeled calcite $\delta^{18}O$ from Karstolution, but with an enrichment of ~1% (**Figure 6B**), which would be expected if the $\delta^{18}O$ are impacted by in-cave kinetic effects. Additionally, the calcite $\delta^{18}O$ compositions from CP reveal an enrichment from the center of the watch glass to the edge of the calcite on the watch glass (**Figure 7B**) a finding consistent with the hypothesis proposed by many others that in-cave kinetic effects lead to variable $\delta^{18}O$ of calcite away from the center of stalagmite growth (Hendy, 1971; Mickler et al., 2006; Tremaine et al., 2011; Riechelmann et al., 2013). Consequently, we propose that stalagmite paleoclimate records developed from these sites in the future be used as records of seasonal ventilation or airflow in the cave system but should be treated with caution as records of precipitation $\delta^{18}O$ and temperature.

We further modeled drip-water $\delta^{18}O$ for the central Sierran foothill cave, Black Chasm, using a five-year record of precipitation $\delta^{18}O$ (Oster et al., 2012) and temperature and evaporation data from a corresponding weather station (National Oceanic and Atmospheric Administration (NOAA), 2021). The modeled drip-water $\delta^{18}O$ for Black Chasm agrees with the measured drip-water $\delta^{18}O$ from Black Chasm (**Supplementary Figure S2**) indicating that Black Chasm drip-water $\delta^{18}O$ is not influenced by in-cave dynamics such as low RH or airflow. This is a significant result as it suggests that Black Chasm drip sites are ideal locations for developing stalagmite paleoclimate records of precipitation $\delta^{18}O$ and temperature, as well as site BYHT from Lilburn Cave. Our interpretation is consistent with the original interpretation from Oster et al. (2012) that the cave hydrology, including drip rates, responds immediately (within hours to days) to large precipitation events (Oster et al., 2012). Dampened variability in the modeled drip-water $\delta^{18}O$ compositions for Black Chasm ($-10.5 \pm 0.6\%$), relative to the measured values, is likely due to overrepresentation of mixing in the Karstolution model. The comparison of the modeled and measured drip-water $\delta^{18}O$ compositions from Black Chasm and Lilburn Cave reveal that the seasonal enrichment experienced at two sites (GC and CP)

and Lilburn Cave is not a regional phenomenon but is instead constrained to these two sites. It is important to note that Black Chasm and Lilburn Cave are separated by 2° of latitude and 4,000 ft of elevation. These differences, however, do not lead to observable difference in the overall variability in precipitation $\delta^{18}O$ (**Supplementary Figure S2**). The elevation and latitude could explain the -1.5% difference in dripwater $\delta^{18}O$ as this is consistent with a lapse rate of $-0.35\%/km$. The explanation, however, could equally be a difference in time between the Black Chasm study and the study presented here. The cross-cave comparisons highlight the need to monitor unique cave environments.

Metals as an Emerging Proxy for Variability in Recharge and Onset of the Rainy Season in Mediterranean Climates

The Lilburn Cave drip water compositions indicate that trace metal concentrations (Cu^{2+}, Mn^{2+}, and Fe^{3+}) may be sensitive to hydrologic recharge in the cave system (**Figure 7**). The increase of Cu^{2+}, Mn^{2+}, and Fe^{3+} concentrations in the autumn suggests that Mn^{2+} is responding to the first available recharge to the system either through increase soil mobilization or through a wash through event by increased recharge in the cave or bedrock system. Additionally, we hypothesize that the change in concentrations of Cu^{2+} and Fe from 2018 to 2019 (**Figure 7**) is due to the region of SEKI experiencing a moderate drought in 2018 followed by a period of greater effective moisture in 2019 (PDSI, 2021). Other studies have demonstrated that these metals are transported and measured in drip waters under peak flow conditions due to the observations that humic-derived organic matter binds metals such as Cu^{2+}, Mn^{2+}, and Fe^{3+} and aides in their transport to the drip site (Hartland et al., 2011; Hartland et al., 2012). We propose that Mn^{2+}, Cu^{2+}, and Fe^{3+} concentrations in drip waters may be a sensitive proxy of recharge intensity and of the onset of the wet season after dry summer months or following a prolonged drought.

These metals can also be concentrated in soils during fire events (Treble et al., 2016) and/or be transported into the cave at a higher rate directly after fire events due to increased recharge

(Treble et al., 2016). Although we know of no proximal fires in the SEKI region during the monitoring period, a controlled burn in Redwood Canyon (2016) may have contributed increased Cu, Mn, and Fe concentrations in the soil above Lilburn Cave. Additionally, the Ferguson Fire (96,901 acres) occurred in Yosemite National Park (~160 km away) in summer 2018, potentially leading to increased aerosols that were transported to SEKI, such as found in other studies (Tadros et al., 2019). Although further work is needed to better understand the transport of trace metals in California cave systems, the observed seasonal trends of these trace metals in Lilburn drip waters and the strong correlation to variability in precipitation amount indicate that increases in the concentrations of these trace metals in drip waters may capture the onset of the rainy season in CA caves. If this hypothesis is shown by further study to be correct, then concentrations of these trace metals in stalagmites would be a critical proxy for reconstructing variability in the timing of the onset of the rainy season in CA, which has been strongly linked to the duration of the fire season (Lukovic et al., 2021; Swain 2021). Moreover, the concentrations of Mn, Cu, and Fe are recorded in the "farmed" calcite from Lilburn Cave at the same levels as they are measured in drip water. The results of this study, despite spanning only 2 years, document that many monitored variables respond to seasonal variability in precipitation amount and temperature. The monitoring results further demonstrate the potential for Lilburn Cave to archive a longer-term record of seasonal variability in stalagmites. Future studies of stalagmites from southern Sierra Nevada caves will benefit from the monitoring study presented in this paper.

SUMMARY

Cave monitoring is a crucial practice to develop and understand paleoclimate reconstructions from speleothems. This study provides a monitoring framework that is applicable to stalagmite studies from seasonally dry karst systems both inside and outside of CA. In this study, we demonstrated that the TE/Ca ratios in Lilburn Cave drip-water and calcite are sensitive to seasonal variability in precipitation amount suggesting that Lilburn Cave speleothems have the potential to accurately record seasonal precipitation changes through time. Additionally, the $\delta^{18}O$ compositions of drip-water at one site is sensitive to precipitation $\delta^{18}O$, however, at two other sites the $\delta^{18}O$ primarily reflects in-cave dynamics, highlighting the need to monitor multiple sites within one cave. Furthermore, trace metals in drip-water from Lilburn Cave are potentially sensitive to the onset of the rainy season in SEKI. Based on this cave monitoring effort, we posit that trace metals and elements are capable of resolving the ambiguity present in studies that focus on paleoclimate reconstructions using $\delta^{18}O$ from speleothems in semi-arid environments. Despite a clear research interest in monitoring the impacts of seasonality on drip-water composition in semi-arid environments, there is to date a relative paucity of monitoring studies for CA karst systems. The results from this study will better inform future work that seeks to provide seasonal context to interpretations drawn from proxy records of stalagmites. Finally, cave and precipitation monitoring studies are an excellent avenue for undergraduate research theses that increase students' retention of geochemical concepts through hands-on learning in the field and the lab.

DATA AVAILABILITY STATEMENT

The original contributions presented in the study are included in the article/**Supplementary Material**, further inquiries can be directed to the corresponding authors.

AUTHOR CONTRIBUTIONS

BW designed the project, did some of the sampling, some of the analysis, wrote the manuscript, and supervised all other analyses. IM aided in the project design, oversight, and manuscript writing and editing. KB, DK, NC, EB, and AP aided in sampling and in analyses. JT aided in project conceptualization and design as well as in permitting and processes related to the National Park. GR-B aided in sampling and project conceptualization.

FUNDING

ACKNOWLEDGMENTS

SUPPLEMENTARY MATERIAL

The Supplementary Material for this article can be found online at: https://www.frontiersin.org/articles/10.3389/feart.2021.781526/full#supplementary-material

REFERENCES

Baker, A., Hartmann, A., Duan, W., Hankin, S., Comas-Bru, L., Cuthbert, M. O., et al. (2019). Global Analysis Reveals Climatic Controls on the Oxygen Isotope Composition of Cave Drip Water. *Nat. Commun.* 10 (1), 1–7. doi:10.1038/s41467-019-11027-w

Banner, J. L., Guilfoyle, A., James, E. W., Stern, L. A., and Musgrove, M. (2007). Seasonal Variations in Modern Speleothem Calcite Growth in Central Texas, U.S.A. *J. Sediment. Res.* 77, 615–622. doi:10.2110/jsr.2007.065

Bian, F., Coleborn, K., Flemons, I., Baker, A., Treble, P. C., Hughes, C. E., et al. (2019). Hydrological and Geochemical Responses of Fire in a Shallow Cave System. *Sci. Total Environ.* 662, 180–191. doi:10.1016/j.scitotenv.2019.01.102

Carlson, P. E., Noronha, A. L., Banner, J. L., Jenson, J. W., Moore, M. W., Partin, J. W., et al. (2020). Constraining Speleothem Oxygen Isotope Disequilibrium Driven by Rapid CO2 Degassing and Calcite Precipitation: Insights from Monitoring and Modeling. *Geochimica et Cosmochimica Acta* 284, 222–238. doi:10.1016/j.gca.2020.06.012

Caprio, A. C., and Lineback, P. (1997). "Interannual Variability of Rock Glacier Flow Velocities in the European Alps," in Proceedings of the Conference on Fire in California Ecosystems: Integrating Ecology, Prevention, and Management, San Diego, CA, November 17–20, 1997.

Casteel, R. C., and Banner, J. L. (2015). Temperature-Driven Seasonal Calcite Growth and Drip Water Trace Element Variations in a Well-Ventilated Texas Cave: Implications for Speleothem Paleoclimate Studies. *Chem. Geology.* 392, 43–58. doi:10.1016/j.chemgeo.2014.11.002

Dreybrodt, W., and Deininger, M. (2014). The Impact of Evaporation to the Isotope Composition of DIC in Calcite Precipitating Water Films in Equilibrium and Kinetic Fractionation Models. *Geochimica et Cosmochimica Acta* 125, 433–439. doi:10.1016/j.gca.2013.10.004

Dreybrodt, W., and Scholz, D. (2011). Climatic Dependence of Stable Carbon and Oxygen Isotope Signals Recorded in Speleothems: from Soil Water to Speleothem Calcite. *Geochimica et Cosmochimica Acta* 75 (3), 734–752. doi:10.1016/j.gca.2010.11.002

Earman, S., Campbell, A. R., Phillips, F. M., and Newman, B. D. (2006). Isotopic Exchange between Snow and Atmospheric Water Vapor: Estimation of the Snowmelt Component of Groundwater Recharge in the Southwestern United States. *J. Geophys. Res.* 111 (D9), D09302. doi:10.1029/2005JD006470

Fairchild, I., and Baker, A. (2012). *Speleothem Science: From Process to Past Environments*. Oxford: Wiley-Blackwell.

Fairchild, I. J., and Treble, P. C. (2009). Trace Elements in Speleothems as Recorders of Environmental Change. *Quat. Sci. Rev.* 28 (5-6), 449–468. doi:10.1016/j.quascirev.2008.11.007

Fairchild, I. J., Borsato, A., Tooth, A. F., Frisia, S., Hawkesworth, C. J., Huang, Y., et al. (2000). Controls on Trace Element (Sr-Mg) Compositions of Carbonate Cave Waters: Implications for Speleothem Climatic Records. *Chem. Geology.* 166, 255–269. doi:10.1016/S0009-2541(99)00216-8

Hartland, A., Fairchild, I. J., Lead J. R., M., Zhang, H., and Baalousha, M. (2011). Size, Speciation and Lability of NOM-Metal Complexes in Hyperalkaline Cave Dripwater. *Geochimica et Cosmochimica Acta* 75 (23), 7533–7551. doi:10.1016/j.gca.2011.09.030

Hartland, A., Fairchild, I. J., Lead J. R., M., Borsato, A., Baker, A., Frisia, S., and Baalousha, M. (2012). From Soil to Cave: Transport of Trace Metals by Natural Organic Matter in Karst Dripwaters. *Chemical Geology* 304 , 68–82. doi:10.1016/j.chemgeo.2012.01.032

Feng, W., Casteel, R. C., Banner, J. L., and Heinze-Fry, A. (2014). Oxygen Isotope Variations in Rainfall, Drip-Water and Speleothem Calcite from a Well-Ventilated Cave in Texas, USA: Assessing a New Speleothem Temperature Proxy. *Geochimica et Cosmochimica Acta* 127, 233–250. doi:10.1016/j.gca.2013.11.039

Fleitmann, D., Cheng, H., Badertscher, S., Edwards, R. L., Mudelsee, M., Göktürk, O. M., et al. (2009). Timing and Climatic Impact of Greenland Interstadials Recorded in Stalagmites from Northern Turkey. *Geophys. Res. Lett.* 36 (19), L19707. doi:10.1029/2009GL040050

Goss, M., Swain, D. L., Abatzoglou, J. T., Sarhadi, A., Kolden, C. A., Williams, A. P., et al. (2020). Climate Change Is Increasing the Likelihood of Extreme Autumn Wildfire Conditions across California. *Environ. Res. Lett.* 15, 094016. doi:10.1088/1748-9326/ab83a7

Hendy, C. H. (1971). The Isotopic Geochemistry of Speleothems-I. The Calculation of the Effects of Different Modes of Formation on the Isotopic Composition of Speleothems and Their Applicability as Palaeoclimatic Indicators. *Geochimica et Cosmochimica Acta* 35 (8), 801–824. doi:10.1016/0016-7037(71)90127-X

Lachniet, M. S. (2009). Climatic and Environmental Controls on Speleothem Oxygen-Isotope Values. *Quat. Sci. Rev.* 28 (5-6), 412–432. doi:10.1016/j.quascirev.2008.10.021

Liao, J., Hu, C., Li, X., and Ruan, J. (2021). Drying Increases Organic Colloidal Mobilization in the Karst Vadose Zone: Evidence from A 15-year Cave-Monitoring Study. *Hydrological Processes* 35 (4), e14163. doi:10.1002/hyp.14163

Lukovic, J., Chiang, J. C. H., Blagojevic, D., and Sekulic, A. (2021). A Later Onset of the Rainy Season in California. *Geo. Phy. Res. Lett.* 48 (4), e2020GL090350. doi:10.1029/2020GL090350

Luo, W., Wang, S., Zeng, G., Zhu, X., and Liu, W. (2014). Daily Response of Drip Water Isotopes to Precipitation in Liangfeng Cave, Guizhou Province, SW China. *Quat. Int.* 349, 153–158. doi:10.1016/j.quaint.2014.01.043

Markowska, M., Baker, A., Treble, P. C., Andersen, M. S., Hankin, S., Jex, C. N., et al. (2015). Unsaturated Zone Hydrology and Cave Drip Discharge Water Response: Implications for Speleothem Paleoclimate Record Variability. *J. Hydrol.* 529 (2), 662–675. doi:10.1016/j.jhydrol.2014.12.044

McCabe-Glynn, S., Johnson, K. R., Strong, C., Zou, Y., Yu, J.-Y., Sellars, S., et al. (2016). Isotopic Signature of Extreme Precipitation Events in the Western U.S. And Associated Phases of Arctic and Tropical Climate Modes. *J. Geophys. Res. Atmos.* 121 (15), 8913–8924. doi:10.1002/2016JD025524

McDermott, F. (2004). Palaeo-Climate Reconstruction from Stable Isotope Variations in Speleothems: A Review. *Quat. Sci. Rev.* 23 (7-8), 901–918. doi:10.1016/j.quascirev.2003.06.021

McDonough, L., Treble, P., Baker, A., Borsato, A., Frisia, S., Nagra, G., et al. (2021). Past Fires and Post-Fire Impacts Reconstructed from a Southwest Australian Stalagmite. *EarthArXiv.* doi:10.31223/X5JC86

Mickler, P. J., Banner, J. L., Stern, L., Asmerom, Y., Edwards, R. L., and Ito, E. (2004). Stable Isotope Variations in Modern Tropical Speleothems: Evaluating Equilibrium vs. Kinetic Isotope Effects. *Geochimica et Cosmochimica Acta* 68, 4381–4393. doi:10.1016/j.gca.2004.02.012

Mickler, P. J., Stern, L. A., and Banner, J. L. (2006). Large Kinetic Isotope Effects in Modern Speleothems. *Geol. Soc. America Bull.* 118 (1-2), 65–81. doi:10.1130/B25698.1

Mickler, P. J., Carlson, P., Banner, J. L., Breecker, D. O., Stern, L., and Guilfoyle, A. (2019). Quantifying Carbon Isotope Disequilibrium during In-Cave Evolution of Drip Water along Discreet Flow Paths. *Geochimica et Cosmochimica Acta* 244, 182–196. doi:10.1016/j.gca.2018.09.027

Mosenfelder, J., Bosted, P., Hacker, B., Despain, J., and Tinsley, J. Personnel of the Cave Research Foundation (2018). Lilburn Cave Map. *Cave Research Foundation*. Sequoia/Kings Canyon Operations Area.

Nagra, G., Treble, P. C., Andersen, M. S., Fairchild, I. J., Coleborn, K., and Baker, A. (2016). A post-Wildfire Response in Cave Dripwater Chemistry. *Hydrol. Earth Syst. Sci.Earth Syst.Sci.* 20, 2745–2758. doi:10.5194/hess-20-2745-2016

National Oceanic and Atmospheric Administration (NOAA) (2021). California Nevada River Forecast Center. Monthly Precipitation Summary for 2018, 2019, and 2020 for Grant Grove and New Melones Dam HQ. Available at: https://www.cnrfc.noaa.gov/monthly_precip_2019.php (Accessed March, 2021).

Oster, J. L., Montañez, I. P., and Kelley, N. P. (2012). Response of a Modern Cave System to Large Seasonal Precipitation Variability. *Geochimica Et Cosmochimica Acta* 91, 92–108. doi:10.1016/j.gca.2012.05.027

Oster, J. L., Montañez, I. P., Mertz-Kraus, R., Sharp, W. D., Stock, G. M., Spero, H. J., et al. (2014). Millennial-Scale Variations in Western Sierra Nevada Precipitation during the Last Glacial Cycle MIS 4/3 Transition. *Quat. Res.* 82 (1), 236–248. doi:10.1016/j.yqres.2014.04.010

Oster, J. L., Montañez, I. P., Santare, L. R., Sharp, W. D., Wong, C., and Cooper, K. M. (2015). Stalagmite Records of Hydroclimate in central California during Termination 1. *Quat. Sci. Rev.* 127, 199–214. doi:10.1016/j.quascirev.2015.07.027

Oster, J. L., Weisman, I. E., and Sharp, W. D. (2020). Multi-Proxy Stalagmite Records from Northern California Reveal Dynamic Patterns of Regional Hydroclimate over the Last Glacial Cycle. *Quat. Sci. Rev.* 241, 106411. doi:10.1016/j.quascirev.2020.106411

Oster, J. L., Sharp, W. D., Covey, A. K., Gibson, J., Rogers, G., and Mix, H. (2017). Climate Response to the 8.2 ka Event in Coastal California. *Scientific Reports* 7 (1), 1–9. doi:10.1038/s41598-017-04215-5

Oster, J. L., Montanez, I. P., Sharp, W. D., and Cooper, K. M. (2009). Late Pleistocene California Droughts During Deglaciation and Arctic Warming. *Earth Planet. Sci. Lett.* 228 (3–4), 434–443. doi:10.1016/j.epsl.2009.10.003

A. DaiNational Center for Atmospheric Research Staff (Editors) (2021). *The Climate Data Guide: Palmer Drought Severity Index (PDSI)*. Retrieved from https://climatedataguide.ucar.edu/climate-data/palmer-drought-severity-index-pdsi.

PRISM Climate Group (2014). *Oregon State University*. Retrieved from https://prism.oregonstate.edu. Accessed on: August 20, 2021.

Riechelmann, D. F. C., Deininger, M., Scholz, D., Riechelmann, S., Schröder-Ritzrau, A., Spötl, C., et al. (2013). Disequilibrium Carbon and Oxygen Isotope Fractionation in Recent Cave Calcite: Comparison of Cave Precipitates and Model Data. *Geochimica et Cosmochimica Acta* 103, 232–244. doi:10.1016/j.gca.2012.11.002

Sinclair, D. J., Banner, J. L., Taylor, F. W., Partin, J., Jenson, J., Mylroie, J., et al. (2012). Magnesium and Strontium Systematics in Tropical Speleothems from the Western Pacific. *Chem. Geology.* 294-295, 1–17. doi:10.1016/j.chemgeo.2011.10.008

Sinclair, D. J. (2011). Two Mathematical Models of Mg and Sr Partitioning into Solution during Incongruent Calcite Dissolution. *Chem. Geology.* 283 (3-4), 119–133. doi:10.1016/j.chemgeo.2010.05.022

Swain, D. L. (2021). A Shorter, Sharper Rainy Season Amplifies California Wildfire Risk. *Geophy. Res. Lett.* 48 (5), e2021GL092843. doi:10.1029/2021GL092843

Tadros, C. V., Treble, P. C., Baker, A., Hankin, S., and Roach, R. (2019). Cave Drip Water Solutes in South-Eastern Australia: Constraining Sources, Sinks and Processes. *Sci. Total Environ.* 651 (2), 2175–2186. doi:10.1016/j.scitotenv.2018.10.035

Tinsley, J. C., Des Marais, D. J., McCoy, G., Rogers, B. W., and Ulfeldt, S. R. (1981). "Lilburn Cave's Contributions to the Natural History of Sequoia and Kings Canyon National Parks, California, USA," in Proceedings of the Eighth International Speleological Congress, Bowling Green, Kentucky, 1, 287–290.

Tobin, B., and Schwartz, B. (2012). Quantifying Concentrated and Diffuse Recharge in Two marble Karst Aquifers: Big Spring and Tufa Spring, Sequoia and Kings Canyon National Parks, California, USA. *J. Cave Karst Stud.* 74 (2), 186–196. doi:10.4311/2011Jcks0210

Treble, P. C., Fairchild, I. J., Baker, A., Meredith, K. T., Andersen, M. S., Salmon, S. U., et al. (2016). Roles of forest Bioproductivity, Transpiration and Fire in a Nine-Year Record of Cave Dripwater Chemistry from Southwest Australia. *Geochimica Et Cosmochimica Acta* 184, 132–150. doi:10.1016/j.gca.2016.04.017

Treble, P., Mah, M., Griffiths, A., Baker, A., Deininger, M., Kelly, B., et al. (2019). Separating Isotopic Impacts of Karst and In-Cave Processes from Climate Variability Using an Integrated Speleothem Isotope-Enabled Forward Model. *Earth ArXiv.* doi:10.31223/osf.io/j4kn6

Tremaine, D. M., Froelich, P. N., and Wang, Y. (2011). Speleothem Calcite Farmed *In Situ*: Modern Calibration of δ18O and δ13C Paleoclimate Proxies in a Continuously-Monitored Natural Cave System. *Geochimica et Cosmochimica Acta* 75 (17), 4929–4950. doi:10.1016/j.gca.2011.06.005

Western Regional Climate Center (WRCC) (2021). Western Monthly Climate Summaries. Available at http://wrcc.dri.edu/Climate/Monthly_Summaries/west_summaries. (Accessed on: August 20, 2021).

Wong, C. I., and Breecker, D. O. (2015). Advancements in the Use of Speleothems as Climate Archives. *Quat. Sci. Rev.* 127, 1–18. doi:10.1016/j.quascirev.2015.07.019

Wong, C. I., Banner, J. L., and Musgrove, M. (2011). Seasonal Dripwater Mg/Ca and Sr/Ca Variations Driven by Cave Ventilation: Implications for and Modeling of Speleothem Paleoclimate Records. *Geochimica et Cosmochimica Acta* 75 (12), 3514–3529. doi:10.1016/j.gca.2011.03.025